Transition State Theory for Multichannel Addition Reactions: Multifaceted Dividing Surfaces

Yuri Georgievskii*,† and Stephen J. Klippenstein*,‡

Combustion Research Facility, Sandia National Laboratories, Livermore, California 94551-0969

Received: March 4, 2003; In Final Form: July 3, 2003

A variational multifaceted dividing surface generalization of the variable reaction coordinate (VRC) approach is described. This approach involves the incorporation and optimization of multiple pivot points for each fragment. Illustrative applications to a variety of barrierless reactions with multiple addition channels are presented. For the addition of H atoms to propargyl radical a high level ab initio potential is employed and comparisons are made with trajectory simulations and with prior implementations of VRC-TST. The multifaceted VRC-TST results agree with the trajectory results to within 5−10% as do prior approximate multifaceted VRC-TST results, obtained via the neglect of the flux through certain connecting surfaces. In contrast, results based on the sums of properly variational single faced results differ significantly, being ∼15−20% greater. Notably, the optimal multifaceted transition state dividing surfaces are again in qualitative accord with contours of the radical molecular orbital. Applications to the $CH_3 + CH_3$ and $C_2H_3 + O_2$ reactions further illustrate the dependence of the results on the use of multiple pivot points, while also illustrating the implementation of directly determined density functional interaction energies. Interestingly, these a priori results are in reasonable agreement with experiment for both these reactions.

I. Introduction

The variable reaction coordinate (VRC) transition state theory (TST) approach[1,2] has proven to be of considerable utility in estimating the kinetics of barrierless additions. Within this approach, the transition state dividing surface is defined by a fixed distance between two pivot points, one for each fragment. The position of each pivot point in the molecular frame of the corresponding fragment effectively determines the shape of the dividing surface. The optimization of the pivot point locations, in addition to the distance between them, often yields a significant reduction relative to optimizations constrained to a single type of dividing surface, such as that provided by a fixed center-of-mass separation.[3−7]

Although the family of dividing surfaces considered in the VRC-TST approach are widely appropriate, there are some instances where further flexibility seems desirable. For instance, consider the addition of an H atom to the radical p-orbital in a radical such as OH. The optimal dividing surface for the H motion in such reactions might be expected to have a toroidal shape with cylindrical symmetry about the OH axis. However, the symmetry requirements in the present VRC-TST formalism restrict the OH fixed point to lie along its linear axis, with the resulting dividing surface having a spherical shape.

Addition reactions where there are multiple binding sites provide another example of a situation where it is desirable to have increased flexibility in the shape of the dividing surface. In particular, for such reactions a dividing surface whose shape can be separately optimized in the regions about each of the binding sites would be expected to provide a significant improvement over a dividing surface whose shape is determined by global considerations of all addition sites. The presence of multiple binding sites is fairly commonplace. For example, they arise in addition reactions of resonantly stabilized radicals such as C_3H_3, O_2, and NO_2, in radical additions where the attack may come from more than one side, such as for CH_3, C_2H_3, C_3H_3, and C_3H_7 additions, and in ion−molecule reactions where the molecule has multiple electrostatic binding sites.

Prior applications of the VRC-TST formalism to such reactions have treated the sites separately and simply summed the individual fluxes to obtain the total flux.[7,8,9] This has been done in both a properly variational manner, where each dividing surface completely enclosed the relevant binding site,[9] and in a more approximate manner, where a division of binding sites is obtained by effectively incorporating an infinite potential barrier between each of the binding sites.[7,8] Although the latter approach yields significant reductions, it introduces a nonvariational character to the calculation, and corresponding uncertainties in its predictions. Furthermore, its implementation is different for each new reaction and requires detailed consideration of the potential energy surface to properly locate the effective barrier.

In this work, we describe and implement a properly variational multifaceted dividing surface approach which allows for the incorporation and optimization of different dividing surface shapes for each separate binding site. As described in section II, this variational approach is a simple generalization of the VRC-TST formalism to include multiple pivot points for each reacting fragment. The formal details of the present implementation of such multifaceted VRC dividing surfaces are provided in section III. Illustrative calculations for the $H + C_3H_3$, $CH_3 + CH_3$, and $C_2H_3 + O_2$ reactions are presented and discussed in section IV. For the $H + C_3H_3$ reaction comparisons with trajectory simulations and with prior variational and nonvariational methodologies are included. For the latter two reactions the results are also briefly compared with experiment. Some concluding remarks are then made in section V.

* Corresponding author.
† E-mail: ygeorgi@sandia.gov.
‡ E-mail: sjklipp@sandia.gov.

10.1021/jp034564b CCC: $25.00
Published on Web 10/25/2003

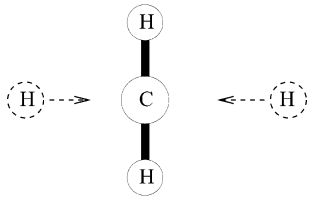

Figure 1. Two ways the hydrogen atom may approach the methyl radical in the $CH_3 + H$ reaction. The plane of the radical is perpendicular to the plane of the picture and the third hydrogen atom is hidden behind the carbon atom.

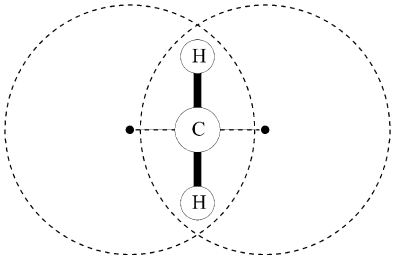

Figure 2. Composite dividing surface for the $CH_3 + H$ reaction.

II. Multifaceted Dividing Surfaces

As a simple but illuminating example one can consider the reaction of a methyl radical with a hydrogen atom,

$$CH_3 + H \rightarrow CH_4 \qquad (1)$$

This reaction may proceed in two (indistinguishable) ways, depending on from which side of the CH_3 plane the hydrogen approaches, Figure 1. In accord with the VRC ideology it would be reasonable to assume that shifting the pivot point along the C_{3v} symmetry axis of the CH_3, from its center of mass position in the direction of the approaching hydrogen, will decrease the flux and improve the rate constant estimate.[10] However, the resulting dividing surface would not be symmetric with respect to reflection over the molecular plane and any decrease in the reactive flux through the front part of the surface (i.e., the part of the surface on the side of the CH_3 plane corresponding to the pivot-point displacement) will be more than balanced by an increase in the reactive flux through the back part of the dividing surface. In prior work, we avoided this difficulty by restricting the angle between the CH_3 C_{3v} symmetry axis (in the direction of the pivot point) and the direction of the vector connecting the CH_3 center of mass with the reactive hydrogen atom to 90° or less.[10] The resulting flux for the front side is then doubled to obtain the total flux.

It is instructive to consider a different perspective to this angle-restricted approach to flux optimization. Namely, the dividing surfaces used for the optimization can be viewed as composite surfaces, consisting of the outer surface of the union of two symmetrically related spheres, Figure 2. One sphere is centered about the fixed point on one side, and the other, which may be obtained by reflection over the CH_3 plane, is centered about an equivalent fixed point on the other side. The two spheres intersect in the CH_3 plane along the circle. With this view there are two pivot points (sphere centers) associated with the methyl radical, one on each side of the CH_3 plane. In the flux calculation, one integrates over only that part of each sphere which is on the same side as its corresponding pivot point. This composite surface can be defined by the following simple condition,

$$\min_{i=1,2} r_i = s' \qquad (2)$$

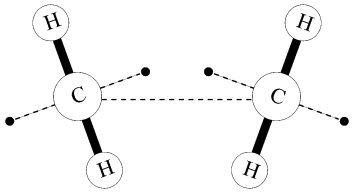

Figure 3. Way the reactants may approach each other in the $CH_3 + CH_3$ reaction.

where r_i, $i = 1, 2$ is the distance between the hydrogen atom and pivot point i and s' is the reaction coordinate value. It is important to note that this composite dividing surface is *continuous* and, therefore, provides a rigorous upper bound for the reaction rate constant.

Now, let us consider a bit more complicated example, namely, the reaction between two methyl radicals,

$$CH_3 + CH_3 \rightarrow C_2H_6 \qquad (3)$$

This reaction may proceed in four different (and indistinguishable) ways, depending on the orientation of the CH_3 radicals with respect to each other, Figure 3. Once again, according to the VRC approach, one should try to position pivot points shifted in the direction of the reaction product. However, one faces the same difficulty as for the $CH_3\cdots H$ reaction that a single pair of the pivot points, one point for each fragment, does not allow one to optimize the flux for all four channels. Intuitively, it is clear that the vector connecting a fragment's center of mass with its pivot point should point in the direction of the other fragment, cf. Figure 3. However, we have not been able to express this condition in terms of restrictions imposed on the angles between appropriate vectors in such a way that the resulting dividing surface is continuous, without holes. Neglecting the flux through these holes, as in our prior work,[11] corresponds to an assumption of an infinite potential barrier in the region of the hole. On the other hand, eq 2 can be easily generalized to the present case,

$$\min_{i=1,j=1}^{2} r_{i,j} = s' \qquad (4)$$

where $r_{i,j}$, $i = 1, 2$, $j = 1, 2$ is the distance between the ith and jth pivot points, associated with the first and second fragment, respectively (each methyl radical having two pivot points, as before). It is easy to see that eq 4 satisfies the qualitative requirement on the fragments orientation described above. The resulting composite surface consists of four standard VRC surface facets, one per each pair of pivot points. Importantly, the constructed surface is continuous.

It is easy to generalize the above considerations to a situation when each fragment has an arbitrary number of pivot points. In this general situation the distances between the pivot points for different pairs of the pivot points need not be the same. As a result, the dividing surface that is characterized by n_1 pivot points associated with the first fragment and n_2 pivot points for the second fragment, as well as by $n_1 \times n_2$ distances $s'_{i,j}$ between the pivot points for different pairs of the pivot points, can be defined as

$$\min_{i=1,j=1}^{n_1,n_2} r_{i,j}/s'_{i,j} = 1 \qquad (5)$$

where $r_{i,j}$, $i = 1, ..., n_1$, $j = 1, ..., n_2$ is the distance between the ith pivot point associated with the first fragment and the jth pivot point associated with the second fragment. The dividing

surface so defined is quite general. It consists of the $n_1 \times n_2$ elementary VRC surfaces, each of which is defined by the condition $r_{i,j} = s'_{i,j}$. Only that part of the i,jth elementary VRC surface is exposed to the flux, for which $r_{i',j'} > s'_{i',j'}$, for all pairs of i' and j' where either $i' \neq i$ or $j' \neq j$. For this reason we call the composite dividing surface defined by eq 5 the multifaceted dividing surface (MDS). Some pairs of the pivot points and the corresponding elementary VRC surfaces can be excluded if one formally sets the corresponding $s'_{i,j}$ distances to have negative values. Importantly, the dividing surface defined by eq 5 is again continuous and, therefore, provides a rigorous upper bound for the classical rate constant.

The MDS allows one to treat reactions with multiple channels for any combination of atomic, linear, and nonlinear fragments. In this aspect it is interesting to note that even though the concept of the MDS was developed independently, it may serve as a natural generalization of the "snowman" dividing surface, discussed recently by Robertson et al.,[9] to the case when both fragments participating in the reaction are polyatomic.

The implementation of a MDS-VRC approach is straightforward when the calculation of the flux through such a dividing surface is performed with a Monte Carlo sampling method.[2,12] In particular, it simply requires a homogeneous sampling of each i,jth elementary VRC surface belonging to the multifaceted dividing surface with the same approach employed in the standard single surface VRC approach.[12] Only those samplings are accepted for which $r_{i',j'} > s'_{i',j'}$, for all pairs of i' and j' with either $i' \neq i$ or $j' \neq j$.

III. Methodology

The E,J-resolved variational TST expression for the high-pressure recombination rate constant $k(T)$ at the temperature T can be written as[13]

$$k(T) = \frac{1}{2\pi} g_e \frac{\sigma_1 \sigma_2}{\sigma^\dagger} \left(\frac{2\pi}{\mu k_B T}\right)^{3/2} \frac{\int \mathrm{d}E\, \mathrm{d}J\, N^\dagger(E,J) \mathrm{e}^{-E/k_B T}}{\mathrm{Q}_1(T)\, \mathrm{Q}_2(T)} \quad (6)$$

where g_e is the electronic degeneracy factor and σ_1, σ_2, and $\sigma^\dagger$ are the rotational symmetry numbers for the reactants and transition state, respectively. The quantity $\mu = m_1 m_2/(m_1 + m_2)$ is the reduced mass, Q_1 and Q_2 are the partition functions of the reactants, which are treated classically with respect to rotational degrees of freedom. $N^\dagger(E,J)$ is the E and J resolved number of states, $N(E,J)$, of the reactive complex, which is minimized over the dividing surface for each pair of values of the energy E and the total angular momentum J. Here and further we use atomic units, in which $\hbar = 1$.

The classical expression for $N(E,J)$ can be written as[14]

$$N(E,J) = (2\pi)^{1-\nu} \int \mathrm{d}^\nu Q\, \mathrm{d}^\nu P\, \delta(s(Q) - s')\, \delta(H(Q,P) - E)\, \delta(\hat{J}(Q,P) - J) \dot{s} \Theta(\dot{s}) \quad (7)$$

where Q and P are ν-dimensional generalized coordinates and momenta, the dividing surface is defined in terms of a fixed value s' for the "reaction coordinate" $s(Q)$, the dynamical variable for the total angular momentum is denoted as $\hat{J}$, whereas its numerical value is denoted as J, Θ is the Heaviside step function, and the dot denotes the time derivative, $\dot{s} \equiv \mathrm{d}s/\mathrm{d}t$.

To simplify calculations, we consider only the contribution to $N(E,J)$ from the transitional modes, i.e., that from the rotations and relative translations. The contribution to $N(E,J)$ from the fragment vibrational degrees of freedom can be shown to be equivalent under reasonable limiting assumptions (i.e., vibrational adiabaticity for the conserved modes coupled with invariant conserved mode vibrational frequencies) to their contribution to the reactant partition functions, Q_1 and Q_2, and thus cancel out.[15]

Our recently described methodology for the calculation of the transitional mode contribution to $N(E,J)$ within the standard single surface VRC approach[12] provides the basis for the present evaluations. The expression for $N(E,J)$, eq 7 can be rewritten in the following form,

$$N(E,J) = \langle N_q(E,J,Q) \rangle_\Omega \quad (8)$$

$$N_q(E,J,Q) = \frac{1}{\pi^{3-k_a}} s'^2 \int \mathrm{d}^\nu P\, \delta(H(Q,P) - E)\, \delta(\hat{J}(Q,P) - J) \dot{s} \Theta(\dot{s}) \quad (9)$$

where $\langle \cdots \rangle_\Omega = \int \ldots \mathrm{d}\Omega^{(1)}\, \mathrm{d}\Omega^{(2)}\, \mathrm{d}\Omega^{(12)} / \int \mathrm{d}\Omega^{(1)}\, \mathrm{d}\Omega^{(2)}\, \mathrm{d}\Omega^{(12)}$ denotes the homogeneous averaging over all possible orientations of the fragments and of the vector $\boldsymbol{s}$ (of length s') connecting the fragments pivot points and $k_a = 0$, 1 is the number of monatomic fragments. The integration over the generalized momenta in eq 9 can be performed analytically, giving as a result a relatively simple expression, which can be straightforwardly evaluated.[12,16]

To perform the averaging in eq 8, the crude Monte Carlo sampling method can be used,[12]

$$N(E,J) = M^{-1} \sum_{i=1}^{M} N_q(E,J,Q_i) \quad (10)$$

where M is the total number of samplings. In the case of the specific VRC surface being a part of the MDS, eq 8 should be modified to take into account that only a part of the VRC surface is exposed to the flux,

$$N(E,J) = F \langle N_q(E,J,Q) \rangle_\Omega \quad (11)$$

where F is the fraction of the VRC surface exposed to the flux and the average of N_q over Ω is evaluated over only that portion of the VRC surface exposed to the flux. Using the Monte Carlo sampling method it can be written as

$$F = M'/M \quad (12)$$

where M' is the number of accepted samplings (see the discussion after eq 5). As a result, the following operational expression for the number of states $N(E,J)$ associated with any one particular VRC surface facet in the MDS is obtained,

$$N(E,J) = M^{-1} \sum_{i=1}^{M'} N_q(E,J,Q_i) \quad (13)$$

The use of additional pivot points within the MDS formalism makes the dividing surface more flexible and, thereby, improves the VTST estimate for the reaction rate constant. However, this increased flexibility comes at the cost of increased calculation time, because the flux must be evaluated for each individual dividing surface. In particular, with the MDS approach one must consider a range of dividing surfaces for each of the faces (typically 10 or more surfaces spanning separations from 2 to 6 Å for each face). If global surfaces are generated as the direct product of the surfaces for each of the faces, then the computational effort scales as the power of the number of faces considered. When analytic potentials are available, the flux through any one surface can be obtained with less than 1 min of CPU on a PC. Thus, in that case, the consideration of the

direct product of multiple surfaces for each face is readily feasible but can yield CPU times that are of the same order of magnitude as trajectory simulations. In contrast, when an analytic form for the potential is not available, the direct potential evaluation becomes the determining factor in the computational efficiency. For the methyl radical recombination the direct evaluation of the reactive flux through a single surface at an accuracy of a few percent requires CPU times on the order of 10 h on a 32-node Alpha cluster with ev56 processors. Fortunately, the optimal dividing surfaces for the separate faces are generally closely correlated and one can consider only a limited portion of the direct product set. Furthermore, symmetry implies that the optimal dividing surface for one face is equivalent to that for any symmetrically related faces. In general, we have found that reasonably optimized global dividing surfaces can be obtained via the consideration of about 3−5 times as many dividing surfaces as are required for the single-faced results. Nevertheless, the optimal number of pivot points and pivot point separations is, necessarily, a compromise between the required accuracy and the available computational resources. Various strategies were employed to reduce the computational effort involved in obtaining the optimal dividing surfaces for the full range of energy and angular momentum. In each instance, the flux minimization is performed on a finite set of dividing surfaces corresponding to a grid of pivot point locations and separations.

For comparison purposes, for the $H + C_3H_3$ reaction we have also performed trajectory simulations of the capture process employing Keck's method of initiating trajectories at an approximate transition state dividing surface.[17] A brief description of our implementation of this methodology has been provided in ref 10 and a more detailed exposition will be provided in a forthcoming article. For now we simply note that the trajectories were initiated at the canonically optimized VRC dividing surface and were deemed to have reacted upon reaching certain minimal distances, 3 or 3.5 bohr, between the hydrogen atom and the radical C atoms associated with the propargyl radical, and to have returned to reactants upon reaching center-of-mass separations of 13 bohr or greater.

IV. Results and Discussion

A. $H + C_3H_3$. In this section we apply the multifaceted dividing surface (MDS) approach to the addition of an H atom to a propargyl radical. This addition can occur to either the CH or the CH_2 side of the propargyl radical to yield either allene or propyne:

$$C_3H_3 + H \rightarrow \begin{cases} CH_2CCH_2 \\ CHCCH_3 \end{cases} \qquad (14)$$

The addition can also occur from either above or below the plane of the propargyl radical (cf. Figure 4 from ref 8). Thus, four separate pivot points are considered in the application of the MDS approach to this reaction. The comparison of the MDS results with both trajectory simulations and standard single-faced VRC approaches for this reaction serves to illustrate the utility of the MDS approach as well as any limitations in the standard approaches. The analytic potential from ref 8, which is based on multireference configuration interaction calculations was employed in each of these calculations.

Three sets of dividing surfaces were considered. For each set, a single pivot point associated with the H fragment was always taken to coincide with its center of mass. In the first set

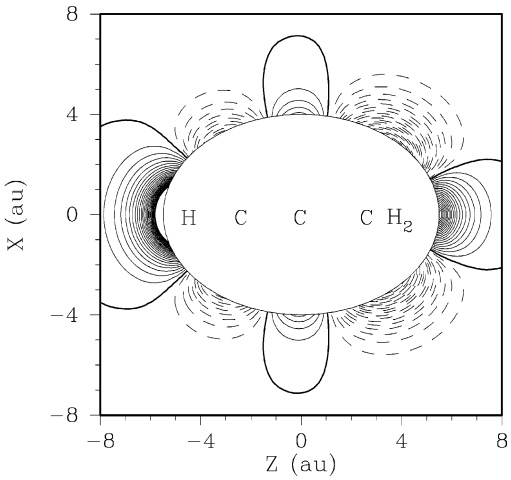

Figure 4. Two-dimensional cut of the three-dimensional surface for the $H + C_3H_3$ reaction. The plotting plane is perpendicular to the plane of the C_3H_3 radical and bisects the HCH angle. Solid contours are positive, dashed contours negative, and the zero-energy contour (defined to be the energy of $H + C_3H_3$) is shown with a heavy solid line. The contour increment is 2 kcal/mol.

the standard VRC surface was considered with a single pivot point associated with the propargyl radical. Because of the symmetry of the propargyl radical, this single pivot point lay along the CC axis. The *z* value for this pivot point, describing the location relative to the central C atom (cf. Figure 4), was varied from 0 to 1 bohr with a 0.25 bohr step. The dividing surface radius *s* was varied in the range from 4 to 13 bohr with a step of 0.25 bohr. It was found that the optimal position of the pivot point is close to $z = 0.5$ for most values of the energy and total angular momentum.

In the second set four pivot points were associated with the propargyl radical. The symmetry of the molecule dictates that the dividing surface should be symmetric relative to the molecular plane and to the plane perpendicular to the molecular plane and passing through the C−C−C axis. Preliminary calculations showed that the optimal positions of the pivot points are approximately energy and angular momentum independent. Thus, to reduce the computational work in the final evaluations, we set the coordinates of these pivot points to $x = \pm 1.5$, $y = 0$, and $z = \pm 2$, which are close to their optimal values. These pivot point locations provide dividing surfaces that correlate closely with the contours of the radical orbitals.[7] The radii of the primitive VRC surfaces were varied from 2.75 to 13 with a step of 0.25.

The results of the calculation of the *E*,*J*-resolved reaction rate constant with these two sets of dividing surfaces are shown in Figure 5. The results of the trajectory calculations are also shown for reference purposes. One can see that the use of a multifaceted dividing surface yields a considerable improvement (∼30%) over the standard single faced VRC surface and agrees with the trajectory result to within 5−10%.

In the third set four pivot points were again associated with the propargyl radical. Now, however, the total flux is evaluated as the sum of the individual fluxes through each of the dividing surfaces; i.e., the overlapping nature of the dividing surfaces is ignored as in the work of Robertson et al.[9] This result is again truly variational, but as can be seen from Figure 5, provides less improvement over the single surface result, especially at low temperatures. In these calculations, the pivot points on either side of the propargyl radical were positioned relative to the nearest carbon atom. The vector **d** connecting the pivot point P

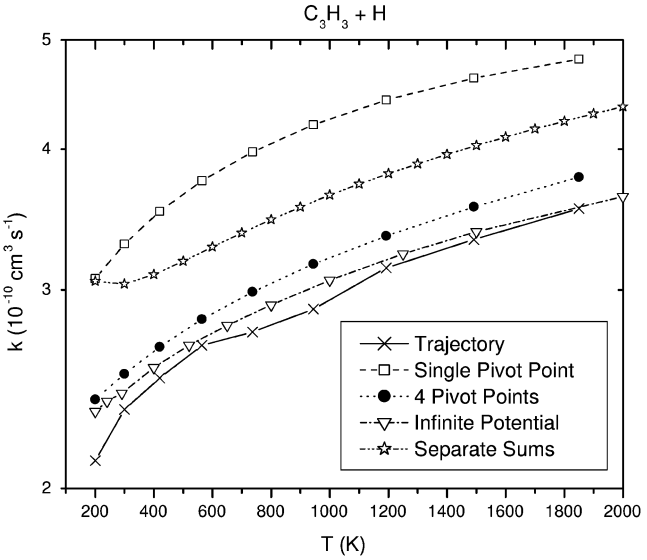

Figure 5. *E, J*-resolved VTST high-pressure rate constant for the reaction $C_3H_3 + H \rightarrow C_3H_4$ is shown as a function of temperature. The results are presented for the standard single pivot point optimization, for the four pivot point optimization, for the cumulative flux through four individual dividing surfaces, for the infinite barrier approximation, and for trajectory simulations.

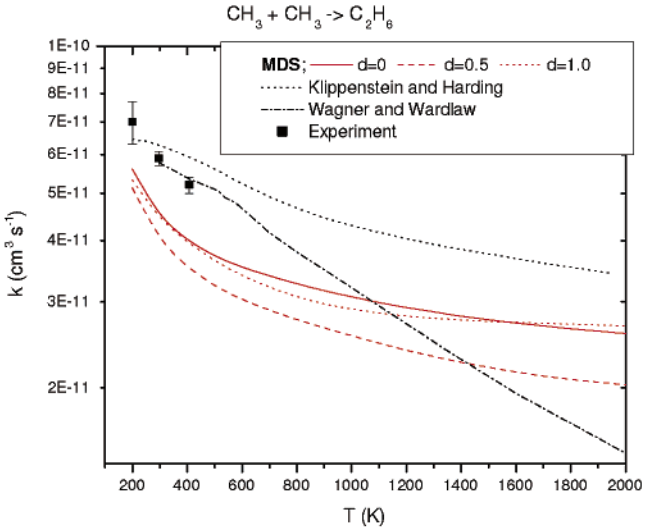

Figure 6. *E, J*-resolved VTST high-pressure rate constant for the $CH_3 + CH_3$ recombination reaction is shown as a function of temperature for a variety of pivot point locations. A variety of related theoretical and experimental results are also plotted.

and the corresponding carbon atom was represented in terms of its length d and the angle ϕ with the C−C axis (the plane P−C−C was perpendicular to the propargyl plane). The length d was varied in the range 0.5−7 bohr with a 0.5 bohr step, and the angle ϕ, from 90° to 150° with a 15° step. The radius r of each surface was varied from 2.5 to 13 bohr with a variable step (0.5 at small r, up to 2 bohr at large r).

For comparison purposes the results of the calculations from ref 8 are also provided in Figure 5. These calculations effectively assumed infinite potential barriers between the CH_2 and CH addition channels, which introduces some nonvariational character to the calculation. This assumption, coupled with the symmetry with respect to the plane of the radical, allows the four channels to be treated separately. The good agreement between these calculations and the four pivot point MDS results indicate that the flux through the assumed barrier is indeed negligible. In fact, the minor deviations between the two results may simply be indicative of minor differences in the details of the two calculations, such as the numbers of pivot points and pivot point separations considered, and the convergence of the Monte Carlo evaluations.

B. $CH_3 + CH_3$. As discussed in section II, the $CH_3 + CH_3$ reaction provides another interesting test case for the use of MDS's. For this reaction four pivot points are again considered; one on either side of each CH_3 radical, with each pivot point directed along the C_{3v} axis. We consider the variation in the MDS predictions with the separation d between the pivot points and their reference C atom. For each d value, a grid of pivot point to pivot point separations s' were considered, with a grid spacing of 0.4 bohr in each instance. For d values of 0, 0.5, and 1.0 bohr the grids of s' covered the range from 4.4 to 7.2 bohr, from 3.0 to 6.2 bohr, and from 2.0 to 5.2 bohr, respectively.

In the absence of a highly accurate analytic potential, we evaluate the potential directly from density functional simulations. We employ the 6-311G** basis set[18] and the B3LYP functional[19] using the Gaussian98 quantum chemistry software.[20] Interaction energies are obtained as the minimum of two separate calculations. One employs the standard initial guess for the wave function whereas the other employs *guess=mix*. A maximum of 1000 configurations were sampled for each dividing surface, which yielded Monte Carlo integration error bars of about 7 for the canonical partition functions. The error bars for *E,J*-resolved calculations are likely even lower.

The results of the present *E,J*-resolved MDS direct VTST calculations are provided in Figure 6. The results for $d = 0.5$ are seen to be significantly lower (as much as 20−30%) than those for either $d = 0$ or $d = 1.0$. This optimum value for d of 0.5 bohr again provides a good correlation between the shape of the dividing surface and the contours of the radical orbitals.[7] Interestingly, the results are also in fairly reasonable agreement with both the high-pressure limit experimental results[21−23] and the previous direct statistical treatment of ref 11, which was based on much higher level multireference configuration interaction ab initio estimates. The flexible TST results from Wagner and Wardlaw,[24] which are based on an empirical potential, are also plotted, because they represent a reasonable extrapolation to the high-pressure limit of a variety of experimental results obtained at higher temperatures.

C. $C_2H_3 + O_2$. For the $C_2H_3 + O_2$ reaction we are interested in considering whether the optimum pivot point for the O_2 group moves away from its center-of-mass, because the addition is ultimately localized to one particular O atom. Thus, for O_2 we consider two pivot points with these pivot points symmetrically displaced from the center-of-mass by a distance d along the linear axis. For simplicity only one pivot point is considered for the C_2H_3 radical, and this pivot point is located at the C atom on the CH side. However, we should note that our prior work for the $C_2H_3 + H$ reaction suggests that some further variational reduction would be obtained by including two separate pivot points for the C_2H_3 radical as well, to account for the addition from either side of the CH portion of the radical.[7,12] We again consider the variation in the MDS predictions with the value of d. For d values of 0 and 0.5 bohr, pivot point to pivot point separations s' ranging from 4.0 to 6.8 bohr were considered, with a grid spacing of 0.2 bohr below 5.2 and 0.4 bohr above. For $d = 1.0$ bohr, an additional grid point at 3.8 bohr is included.

Once again there is no analytic potential for this reaction and it is interesting to consider how accurate direct density functional based estimates are. We employ the same B3LYP/6-311G**

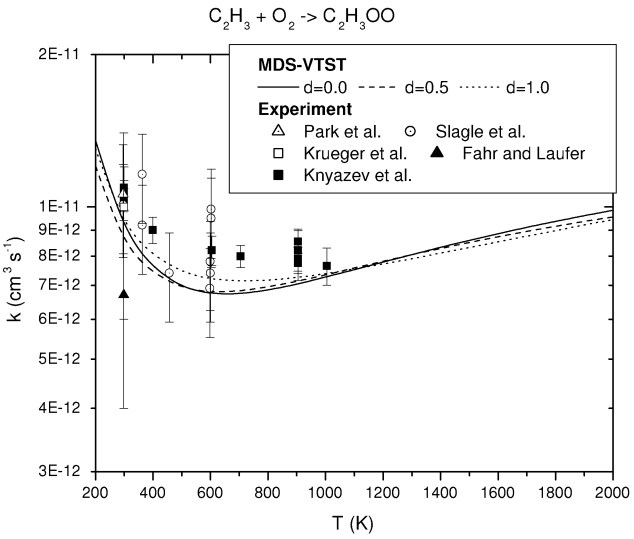

Figure 7. *E*, *J*-resolved VTST high-pressure rate constant for the $C_2H_3 + O_2$ reaction is shown as a function of temperature for a variety of pivot point locations. Related experimental results are also plotted.

scheme and again use the minimum of the energy estimates obtained from the standard guess and from *guess=mix*. Direct samplings of up to 5000 configurations are again used to provide error bars for the canonical rate coefficients of about 7%.

The *E*,*J*-resolved MDS direct VTST predictions for the $C_2H_3 + O_2$ addition rate constant are provided in Figure 7. The modest dependence of the results on *d* is likely related to the fact that the O_2 π orbitals are directed away from the linear axis. Thus, one might imagine the optimal pivot points to be located off the linear axis. However, the cylindrical symmetry of the O_2 molecule does not allow for such an off-axis displacement with the current formalism. The displacements along the axis are unable to reproduce the expected dividing surface shape and the results are fairly insensitive to this parameter. The direct MDS predictions are again in quite reasonable agreement with experiment.[25−29]

V. Concluding Remarks

The present illustrative applications of a multifaceted dividing surface implementation of the variable reaction coordinate approach demonstrate the usefulness of the MDS approach. Appropriate restrictions in pivot point samplings result in a very general methodology that can be widely and efficiently applied. Remarkably, the a priori direct B3LYP/6-311G** based results are in quite satisfactory agreement (maximum deviations of 30%) with experimental results for two quite different types of reactions, i.e., the $CH_3 + CH_3$ and the $C_2H_3 + O_2$ addition reactions.

The present results also suggest that an alternative approach based on the approximate and nonvariational introduction of case specific approximate potential barriers can also be used to obtain meaningful rate constant predictions. In contrast, the simple consideration of sums of variational single surface results tends to yield significant overestimates for the rate constants. Finally, we note that in each instance the optimized multifaceted dividing surfaces appear to be closely correlated to the contours of the radical molecular orbitals.

Acknowledgment. This work was supported by the U.S. Department of Energy, Office of Basic Energy Sciences, Division of Chemical Sciences, Geosciences, and Biosciences. Sandia is a multiprogram laboratory operated by Sandia Corp., a Lockheed Martin Co, for the United States Department of Energy under contract DE-AC04-94-AL85000.

References and Notes

(1) Klippenstein, S. J. *J. Chem. Phys.* **1992**, *96*, 367.
(2) Klippenstein, S. J. *J. Phys. Chem.* **1994**, *98*, 11459.
(3) Klippenstein, S. J. *J. Chem. Phys.* **1991**, *94*, 6469.
(4) Klippenstein, S. J.; Faulk, J. D.; Dunbar, R. C. *J. Chem. Phys.* **1993**, *98*, 243.
(5) Klippenstein, S. J.; East, A. L. L.; Allen, W. D. *J. Chem. Phys.* **1996**, *105*, 118.
(6) Harding, L. B.; Klippenstein, S. J. *Proc. Combust. Inst.* **1998**, *27*, 151.
(7) Klippenstein, S. J.; Harding, L. B. *Phys. Chem. Chem. Phys.* **1999**, *1*, 989.
(8) Klippenstein, S. J.; Harding, L. B. *Proc. Combust. Inst.* **2000**, *28*, 1503.
(9) Robertson, S.; Wagner, A. F.; Wardlaw, D. M. *J. Phys. Chem. A* **2002**, *106*, 2598.
(10) Klippenstein, S. J.; Georgievskii, Y.; Harding, L. B. *Proc. Combust. Inst.* **2002**, *29*, 1229.
(11) Klippenstein, S. J.; Harding, L. B. *J. Phys. Chem. A* **1999**, *103*, 9388.
(12) Georgievskii, Y.; Klippenstein, S. J. *J. Chem. Phys.* **2003**, *118*, 5442. A factor of 2π should be added to all expressions in this paper describing the number of states in the transition state.
(13) Wardlaw, D. M.; Marcus, R. A. *J. Phys. Chem.* **1986**, *90*, 5383.
(14) Miller, W. H. *J. Chem. Phys.* **1976**, *65*, 2216.
(15) Taatjes, C. A.; Klippenstein, S. J. *J. Phys. Chem. A* **2001**, *105*, 8567.
(16) Smith, S. C. *J. Chem. Phys.* **1999**, *111*, 1830.
(17) Keck, J. C. *Adv. Chem. Phys.* **1967**, *13*, 85.
(18) Hehre, W. J.; Radom, L.; Pople, J. A.; v. R. Schleyer, P. *Ab Initio Molecular Orbital Theory*; Wiley: New York, 1987.
(19) Becke, A. D. *J. Chem. Phys.* **1993**, *98*, 5648.
(20) Frisch, M. J.; Trucks, G. W.; Schlegel, H. B.; Scuseria, G. E.; Robb, M. A.; Cheeseman, J. R.; Zakrzewski, V. G.; Montgomery, J. A.; Stratmann, R. E.; Burant, J. C.; Dapprich, S.; Millam, J. M.; Daniels, A. D.; Kudin, K. N.; Strain, M. C.; Farkas, O.; Tomasi, J.; Barone, V.; Cossi, M.; Cammi, R.; Mennucci, B.; Pomelli, C.; Adamo, C.; Clifford, S.; Ochterski, J.; Petersson, G. A.; Ayala, P. Y.; Cui, Q.; Morokuma, K.; Malick, D. K.; Rabuck, A. D.; Raghavachari, K.; Foresman, J. B.; Cioslowski, J.; Ortiz, J. V.; Stefanov, B. B.; Liu, G.; Liashenko, A.; Piskorz, P.; Komaromi, I.; Gomperts, R.; Martin, R. L.; Fox, D. J.; Keith, T.; Al-Laham, M. A.; Peng, C. Y.; Nanyakkara, A.; Gonzalez, C.; Challacombe, M.; Gill, P. M. W.; Johnson, B.; Chen, W.; Wong, M. W.; Andres, J. L.; Gonzalez, C.; Head-Gordon, M.; Replogle, E. S.; Pople, J. A. *Gaussian 98*; Gaussian Inc.: Pittsburgh, PA, 1998.
(21) Hippler, H.; Luther, K.; Ravishankara, A. R.; Troe, J. *Z. Phys. Chem. NF* **1984**, *142*, 1.
(22) Slagle, I. R.; Gutman, D.; Davies, J. W.; Pilling, M. J. *J. Phys. Chem.* **1988**, *92*, 2455.
(23) Walter, D.; Grotheer, H.-H.; Davies, J. W.; Pilling, M. J.; Wagner, A. F. *Proc. Combust. Inst.* **1990**, *23*, 107.
(24) Wagner, A. F.; Wardlaw, D. M. *J. Phys. Chem.* **1988**, *92*, 2462.
(25) Park, J.-Y.; Heaven, M. C.; Gutman, D. *Chem. Phys. Lett.* **1984**, *104*, 469.
(26) Slagle, I. R.; Park, J.-Y.; Heaven, M. C.; Gutman, D. *J. Am. Chem. Soc.* **1984**, *106*, 4356.
(27) Krueger, H.; Weitz, E. *J. Chem. Phys.* **1988**, *88*, 1608.
(28) Fahr, A.; Laufer, A. H. *J. Phys. Chem.* **1988**, *92*, 7229.
(29) Knyazev, V. D.; Slagle, I. R. *J. Phys. Chem.* **1995**, *99*, 2247.